Available online at www.sciencedirect.com
ScienceDirect
International Journal of Heat and Fluid Flow 27 (2006) 955–966
International Journal of HEAT AND FLUID FLOW
www.elsevier.com/locate/ijhff

k–ε Macro-scale modeling of turbulence based on a two scale analysis in porous media

François Pinson [a], Olivier Grégoire [a,*], Olivier Simonin [b]

[a] CEA Saclay, DEN/DM2S/SFME/LETR, 91191 Gif sur Yvette Cedex, France
[b] IMFT, UMR 5502, CNRS/INPT/UPS, Allée du Pr. Camille Soula, 31400 Toulouse, France

Received 27 September 2005; received in revised form 11 January 2006; accepted 4 March 2006
Available online 19 June 2006

Abstract

In this paper, turbulent flows in media laden with solid structures are considered. Following previous studies, we apply both statistical and spatial averages. The solid matrix action on turbulence is then put forward as a sub-filter production. To model this term, we perform a two-scale analysis that highlights energy transfers between the mean motion, the macroscopic and the sub-filter turbulent kinetic energies. Within this framework, we show that the sub-filter production is an energy transfer between the mean motion kinetic energy and the turbulent kinetic energy. We propose to model this sub-filter production using the wake dissipation and the work performed by the mean macroscopic flow against the mean specific drag. From this analysis, a macroscopic k–ε model is then derived for a stratified porous media that includes a friction factor model accounting for turbulence non-equilibrium. Comparisons between this model and a former model [Nakayama, A., Kuwahara, F., 1996. A macroscopic turbulence model for flow in a porous medium. J. Fluid Eng.-T ASME 121, 427–433] are carried out.

Keywords: Porous media; k–ε Model; Wake dissipation; Friction factor; Channel flow; Volume average

1. Introduction

The macroscopic modeling of turbulent flows passing through porous media or media laden with solid structures concerns many practical applications such as nuclear reactors, heat exchangers or canopy flows. In such flows, various study scales coexist. The challenge of the macroscopic modeling is not to reproduce the fine structure dynamics of the flow but to take into account information embedded in smaller scale for large scale modelization. With this aim, we choose to use two average operators: the statistical average that is practical for turbulence study and the spatial average, well adapted for the porous media approach.

It has been shown that constrains apply when using spatial average (Quintard and Whitaker, 1994a,b). If macroscopic quantities length scales are large with respect to the filter size then the spatial average is assumed idempotent. In what follows, $\langle\cdot\rangle$ denotes the volume average, while $\langle\cdot\rangle_f$ is the fluid volume average ($\langle\cdot\rangle \equiv \phi\langle\cdot\rangle_f$), where ϕ is the porosity of the medium. The symbol δ denotes the deviation of a quantity from its fluid averaged value. The statistical average and the fluctuation of some quantity ζ are respectively denoted $\overline{\zeta}$ and ζ'. In a strict mathematical way, both averages commute (Pedras and de Lemos, 2001). However, each modeling step, related to an average application, involves simplifications. Hence, the macroscopic turbulence modelization necessarily depends on the order of application of these two averages (Nield, 2001; Travkin, 2001). Following Pedras and de Lemos (2001), de Lemos and Braga (2003) and also Nakayama and Kuwahara (1996), we choose first to apply the statistical

* Corresponding author. Tel.: +33 1 69 08 22 85; fax: +33 1 69 08 85 68.
E-mail addresses: francois.pinson@cea.fr (F. Pinson), olivier.gregoire@cea.fr (O. Grégoire), olivier.simonin@imft.fr (O. Simonin).

0142-727X/$ - see front matter © 2006 Elsevier Inc. All rights reserved.
doi:10.1016/j.ijheatfluidflow.2006.03.018

average in order to get a structured view of turbulent flows and to benefit from the amount of knowledge available in the literature about RANS modeling. The spatial average is then applied.

Within the framework of the RANS modeling, intensity of the fluctuating motion is usually given by its turbulent kinetic energy (TKE), denoted k. Hence, a practical way to highlight the solid matrix action on turbulence at a macroscopic scale is to study the double averaged balance equation of the turbulent kinetic energy for an incompressible fluid. This equation reads

$$\frac{\mathrm{D}\phi\langle\bar{k}\rangle_{\mathrm{f}}}{\mathrm{D}t} = -\frac{\partial}{\partial x_i}\phi\langle\overline{u_i'k}\rangle_{\mathrm{f}} - \frac{1}{\rho}\frac{\partial}{\partial x_i}\phi\langle\overline{u_i'P'}\rangle_{\mathrm{f}} + \frac{\partial}{\partial x_i}\left(\nu\frac{\partial\phi\langle\bar{k}\rangle_{\mathrm{f}}}{\partial x_i}\right) \underbrace{-\frac{\partial}{\partial x_i}\phi\langle\delta\bar{k}\delta\overline{u_i}\rangle_{\mathrm{f}}}_{\text{dispersion of } \bar{k}} \underbrace{-\phi\left\langle R_{ij}\frac{\partial\overline{u_i}}{\partial x_j}\right\rangle_{\mathrm{f}}}_{\text{spatially filtered shear production}} - \phi\langle\bar{\varepsilon}\rangle_{\mathrm{f}}, \tag{1}$$

where ϕ is the porosity, and $\mathrm{D}\cdot/\mathrm{D}t$ denotes the macroscopic Lagrangian differential operator with respect to the bulk flow velocity. The use of the spatial filter lets the dispersion term appear. This term describes, at a macro-scale, the convective transport of the studied quantity by the local velocity heterogeneities. It is generally modeled by a dispersion tensor (Whitaker, 1967). Using the spatial averaging theorem (Whitaker, 1967) and the filter idempotence, the spatially filtered shear production splits into two contributions

$$-\left\langle R_{ij}\frac{\partial\overline{u_i}}{\partial x_j}\right\rangle_{\mathrm{f}} = -\langle R_{ij}\rangle_{\mathrm{f}}\frac{\partial\langle\overline{u_i}\rangle_{\mathrm{f}}}{\partial x_j} - \left\langle\delta R_{ij}\frac{\partial\delta\overline{u_i}}{\partial x_j}\right\rangle_{\mathrm{f}}. \tag{2}$$

The first contribution is the production term induced by the macro-scale shear. The second term, that we call sub-filter production, and that we note

$$P_{\mathrm{SF}} = -\left\langle\delta R_{ij}\frac{\partial\delta\overline{u_i}}{\partial x_j}\right\rangle_{\mathrm{f}}, \tag{3}$$

is induced by the sub-filter velocity gradients. Therefore, it is directly related to boundary layers at solid surfaces. In this paper, we focus on the modelization of this term.

The analysis of eddies dynamic in porous media led some authors to take into account a supplementary transfer between scales (Finnigan, 2000; Vu et al., 2002). Indeed, large eddies are partially or totally broken by the solid matrix to create small eddies. At macro-scale, this additional spectral transfer competes with the turbulent cascade transfer. Finnigan (2000) underlined that turbulence spectra in forest canopies exhibits a spectral cut-off. Hence a two-scale approach is a natural way to analyse such a turbulent flow owing that the filter length scale is in accordance with the cut-off wave number.

Following this remark, we develop in Section 2 a two-scale analysis (Schiestel, 1987; Grégoire et al., 1999) in order to improve the understanding of energy transfers between scales in porous media. The balance equations for the turbulent kinetic energies and mean motion kinetic energies are introduced. This analysis is then used in Section 3 to derive a macro-scale turbulence model. Modelization of the friction factor is addressed. In the framework of this paper, the flat plate heat exchanger might be seen as an ordered and periodic porous medium. Its study can be reduced to the plane channel one. Fine-scale simulations of plane channel flows are performed and used to tune the macro-scale turbulence model. Comparisons with the model of Nakayama and Kuwahara (1996) are carried out. Encouraging results are shown and possible improvements are proposed.

2. Formal two-scale analysis

2.1. Definitions

Both statistical and spatial averages allow to split up any physical quantity into a mean value and a fluctuation (for the statistical average) or a deviation (for the spatial average). According to the double decomposition concept (Pedras and de Lemos, 2001), based on the formal mathematical commutativity of both average operators, one can write for the ith component of the velocity

$$u_i = \langle\overline{u_i}\rangle_{\mathrm{f}} + \langle u_i'\rangle_{\mathrm{f}} + \delta\overline{u_i} + \delta u_i', \tag{4}$$

where we have by definition:

$$u_i = \bar{u}_i + u_i' \quad \text{and} \quad u_i = \langle u_i\rangle_{\mathrm{f}} + \delta u_i. \tag{5}$$

Various kinetic energies can then be built, depending on the scale under interest. The macro-scale and sub-filter TKE, respectively defined by

$$\bar{k}^{\mathrm{M}} = \overline{\langle u_i'\rangle_{\mathrm{f}}\langle u_i'\rangle_{\mathrm{f}}}/2, \quad \bar{k}^{\mathrm{m}} = \overline{\delta u_i'\delta u_i'}/2, \tag{6}$$

represent the energy which is contained in eddies of characteristic length respectively higher or smaller than the space filter. A cross-scale term may also be defined

$$\bar{k}^{\mathrm{c}} = \overline{\langle u_i'\rangle_{\mathrm{f}}\delta u_i'}/2. \tag{7}$$

This term is not an energy in a strict sense because it is not unconditionally positive.

Let us emphasize that, due to the idempotence property of the spatial average, any macro-scale quantity is equal to its spatially averaged value. Hence, we have

$$\langle\bar{k}\rangle_{\mathrm{f}} = \langle\bar{k}^{\mathrm{M}}\rangle_{\mathrm{f}} + \langle\bar{k}^{\mathrm{m}}\rangle_{\mathrm{f}} = \bar{k}^{\mathrm{M}} + \langle\bar{k}^{\mathrm{m}}\rangle_{\mathrm{f}}. \tag{8}$$

In the same way, one can introduce the macro-scale, sub-filter and cross-scale Reynolds tensors, respectively denoted hereafter $\overline{R}_{ij}^{\mathrm{M}}$, $\overline{R}_{ij}^{\mathrm{m}}$ and $\overline{R}_{ij}^{\mathrm{c}}$

$$\overline{R}_{ij}^{\mathrm{M}} = \overline{\langle u_i'\rangle_{\mathrm{f}}\langle u_j'\rangle_{\mathrm{f}}}, \quad \overline{R}_{ij}^{\mathrm{m}} = \overline{\delta u_i'\delta u_j'}, \quad \overline{R}_{ij}^{\mathrm{c}} = \overline{\langle u_i'\rangle_{\mathrm{f}}\delta u_j'}. \tag{9}$$

One has to notice that $\overline{R}_{ij}^{\mathrm{c}}$ is not symmetric. In addition, let us underline that

$$\bar{k}^{\mathrm{M}} = \overline{R}_{ii}^{\mathrm{M}}/2, \quad \langle\bar{k}^{\mathrm{m}}\rangle_{\mathrm{f}} = \overline{R}_{ii}^{\mathrm{m}}/2. \tag{10}$$

Some authors previously focused on the modelization of the macro-scale quantities $\bar{k}^{\mathrm{M}}$ and $\overline{R}_{ij}^{\mathrm{M}}$ (Antohe and Lage, 1997; Getachew et al., 2000). But these terms do not account for all the turbulence embedded in the media (see discussion of Pedras and de Lemos, 2001).

Lastly, two kinetic energies are defined using the mean velocities, say the macro-scale and sub-filter mean kinetic energies

$$\overline{E}^{\mathrm{M}} = \langle \overline{u_i} \rangle_{\mathrm{f}} \langle \overline{u_i} \rangle_{\mathrm{f}}/2, \quad \langle \overline{E}^{\mathrm{m}} \rangle_{\mathrm{f}} = \langle \delta\overline{u_i} \delta\overline{u_i} \rangle_{\mathrm{f}}/2. \tag{11}$$

2.2. Derivation of the four energies balance equations for a constant porosity medium

On the contrary to Silva and de Lemos (2003) and Breugem and Boersma (2005) that address the issue of the treatment of the interface between free flow and a porous medium, we shall consider in this paper a constant porosity medium. In order to highlight kinetic energy transfers, one may derive balance equations for $\bar{k}^{\mathrm{M}}$, $\langle \bar{k}^{\mathrm{m}} \rangle_{\mathrm{f}}$, $\overline{E}^{\mathrm{M}}$ and $\langle \overline{E}^{\mathrm{m}} \rangle_{\mathrm{f}}$. At first, the balance equation of the four velocities in Eq. (4) are derived

$$\frac{\mathrm{D}\langle \overline{u_i} \rangle_{\mathrm{f}}}{\mathrm{D}t} = -\frac{1}{\rho}\frac{\partial \langle \overline{P} \rangle_{\mathrm{f}}}{\partial x_i} + \frac{\partial}{\partial x_j}\left(\nu \frac{\partial \langle \overline{u_i} \rangle_{\mathrm{f}}}{\partial x_j}\right) - \frac{\partial}{\partial x_j}\langle R_{ij} \rangle_{\mathrm{f}} - \frac{\partial}{\partial x_j}\langle \delta\overline{u_i}\delta\overline{u_j} \rangle_{\mathrm{f}} - \overline{F_{\phi_i}}, \tag{12}$$

$$\frac{\mathrm{D}\langle u_i' \rangle_{\mathrm{f}}}{\mathrm{D}t} = -\frac{1}{\rho}\frac{\partial \langle P' \rangle_{\mathrm{f}}}{\partial x_i} + \frac{\partial}{\partial x_j}\left(\nu \frac{\partial \langle u_i' \rangle_{\mathrm{f}}}{\partial x_j}\right) + \frac{\partial}{\partial x_j}\langle R_{ij} \rangle_{\mathrm{f}} - \frac{\partial}{\partial x_j}\langle \overline{u_i}u_j' \rangle_{\mathrm{f}} - \frac{\partial}{\partial x_j}\langle \delta u_i' \delta u_j \rangle_{\mathrm{f}} - F'_{\phi_i}, \tag{13}$$

$$\frac{\mathrm{D}\delta\overline{u_i}}{\mathrm{D}t} = -\frac{1}{\rho}\frac{\partial \delta\overline{P}}{\partial x_i} + \frac{\partial}{\partial x_j}\left(\nu \frac{\partial \delta\overline{u_i}}{\partial x_j}\right) - \frac{\partial}{\partial x_j}\delta R_{ij} - \frac{\partial}{\partial x_j}(\overline{u_i}\delta\overline{u_j}) + \frac{\partial}{\partial x_j}\langle \delta\overline{u_i}\delta\overline{u_j} \rangle_{\mathrm{f}} + \overline{F_{\phi_i}}, \tag{14}$$

$$\frac{\mathrm{D}\delta u_i'}{\mathrm{D}t} = -\frac{1}{\rho}\frac{\partial \delta P'}{\partial x_i} + \frac{\partial}{\partial x_j}\left(\nu \frac{\partial \delta u_i'}{\partial x_j}\right) + \frac{\partial}{\partial x_j}\delta R_{ij} - \frac{\partial}{\partial x_j}(\overline{u_i}u_j' - \langle \overline{u_i}u_j' \rangle_{\mathrm{f}}) + F'_{\phi_i} - \frac{\partial}{\partial x_j}(\delta u_i'\delta\overline{u_j} + \delta u_i'u_j' + \langle u_i' \rangle_{\mathrm{f}} u_j - \langle u_i'u_j' \rangle_{\mathrm{f}}). \tag{15}$$

where F_{ϕ_i} is the ith component of the specific mean drag (N/kg) of the solid inclusions.

The balance equation for $\bar{k}^{\mathrm{M}}$ is obtained by multiplying the $\langle u_i' \rangle_{\mathrm{f}}$ balance equation (13) by $\langle u_i' \rangle_{\mathrm{f}}$ and by applying the statistical average. This equation can be rewritten to highlight classical terms such as turbulent and molecular diffusions, viscous dissipation and pressure–velocity correlation

$$\frac{\mathrm{D}\bar{k}^{\mathrm{M}}}{\mathrm{D}t} = \underbrace{-\frac{\partial}{\partial x_i}\overline{\langle k^{\mathrm{M}}u_i' \rangle_{\mathrm{f}}}}_{\text{turbulent diffusion of } k^{\mathrm{M}}} \underbrace{-\frac{\partial}{\partial x_i}\overline{\langle k^{\mathrm{c}}u_i' \rangle_{\mathrm{f}}}}_{\text{turbulent diffusion of } k^{\mathrm{c}}} \underbrace{-\frac{1}{\rho}\overline{\frac{\partial \langle u_i' \rangle_{\mathrm{f}} \langle P' \rangle_{\mathrm{f}}}{\partial x_i}}}_{\text{pressure–velocity correlation}} \underbrace{+\frac{\partial}{\partial x_i}\left(\nu\frac{\partial \bar{k}^{\mathrm{M}}}{\partial x_i}\right)}_{\text{molecular diffusion of } \langle \bar{k}^{\mathrm{M}} \rangle_{\mathrm{f}}} \underbrace{-\frac{\partial}{\partial x_i}\langle \bar{k}^{\mathrm{c}}\delta\overline{u_i} \rangle_{\mathrm{f}}}_{\text{dispersion of } \bar{k}^{\mathrm{c}}}$$
$$\underbrace{-\overline{R}_{ij}^{\mathrm{M}}\frac{\partial \langle \overline{u_i} \rangle_{\mathrm{f}}}{\partial x_j}}_{\text{macro-scale shear production}} \underbrace{-\langle \overline{R}_{ij}^{\mathrm{c}}\frac{\partial \delta\overline{u_i}}{\partial x_j} \rangle_{\mathrm{f}}}_{\text{contribution to sub-filter shear production}} \underbrace{-\bar{\varepsilon}^{\mathrm{M}}}_{\text{macro-scale viscous dissipation}} \underbrace{-\overline{\langle u_i' \rangle_{\mathrm{f}} F'_{\phi_i}}}_{\text{work performed by the fluctuant macro-scale velocity against } F'_{\phi}}$$
$$- \underbrace{\left(-\overline{\langle \delta u_j \delta u_i' \rangle_{\mathrm{f}}\frac{\partial \langle u_i' \rangle_{\mathrm{f}}}{\partial x_j}}\right)}_{\text{turbulent cascade through the cut-off wave number}}. \tag{16}$$

The viscous dissipation of macro-scale turbulence is defined thanks to the macroscopic gradient of the fluctuating velocity:

$$\bar{\varepsilon}^{\mathrm{M}} = \nu\overline{\frac{\partial \langle u_i' \rangle_{\mathrm{f}}}{\partial x_j}\frac{\partial \langle u_i' \rangle_{\mathrm{f}}}{\partial x_j}}. \tag{17}$$

In (16), there are two production mechanisms: the shear production in the macro-scale flow and a part of the sub-filter production. Multiplying the $\delta u_i'$ balance equation (15) by $\delta u_i'$ and applying both averages, we derive the $\langle \bar{k}^{\mathrm{m}} \rangle_{\mathrm{f}}$ balance equation

$$\frac{\mathrm{D}\langle \bar{k}^{\mathrm{m}} \rangle_{\mathrm{f}}}{\mathrm{D}t} = \underbrace{-\frac{\partial}{\partial x_i}\langle \overline{k^{\mathrm{m}}u_i'} \rangle_{\mathrm{f}}}_{\text{turbulent diffusion of } k^{\mathrm{m}}} \underbrace{-\frac{\partial}{\partial x_i}\langle \bar{k}^{\mathrm{m}}\delta\overline{u_i} \rangle_{\mathrm{f}}}_{\text{dispersion of } \bar{k}^{\mathrm{m}}} \underbrace{-\frac{1}{\rho}\frac{\partial \langle \overline{\delta u_i'\delta P'} \rangle_{\mathrm{f}}}{\partial x_i}}_{\text{pressure–velocity correlation}} \underbrace{+\frac{\partial}{\partial x_i}\left(\nu\frac{\partial \langle \bar{k}^{\mathrm{m}} \rangle_{\mathrm{f}}}{\partial x_i}\right)}_{\text{molecular diffusion of } \langle \bar{k}^{\mathrm{m}} \rangle_{\mathrm{f}}}$$
$$\underbrace{-\langle \overline{R}_{ij}^{\mathrm{m}} \rangle_{\mathrm{f}}\frac{\partial \langle \overline{u_i} \rangle_{\mathrm{f}}}{\partial x_j}}_{\text{sub-filter shear production}} \underbrace{-\langle (\overline{R}_{ij}^{\mathrm{m}} + \overline{R}_{ji}^{\mathrm{c}})\frac{\partial \delta\overline{u_i}}{\partial x_j} \rangle_{\mathrm{f}}}_{\text{contribution to sub-filter shear production}} \underbrace{-\langle \bar{\varepsilon}^{\mathrm{m}} \rangle_{\mathrm{f}}}_{\text{sub-filter viscous dissipation}} \underbrace{+\overline{\langle u_i' \rangle_{\mathrm{f}} F'_{\phi_i}}}_{\text{work performed by the fluctuant macro-scale velocity against } F'_{\phi}}$$
$$+ \underbrace{\left(-\overline{\langle \delta u_j \delta u_i' \rangle_{\mathrm{f}}\frac{\partial \langle u_i' \rangle_{\mathrm{f}}}{\partial x_j}}\right)}_{\text{turbulent cascade through the cut-off wave number}}. \tag{18}$$

The viscous dissipation of sub-filter turbulence is defined by

$$\bar{\varepsilon}^{\mathrm{m}} = \nu\left\langle \overline{\frac{\partial \delta u_i'}{\partial x_j}\frac{\partial \delta u_i'}{\partial x_j}} \right\rangle_{\mathrm{f}}. \tag{19}$$

The classical spectral transfer induced by the turbulent cascade is recovered. For clear flows, Reynolds et al. (2002)

derived a similar term for the spectral transfer through the cut-off wave number. The work performed by the fluctuating macro-scale velocity against F'_ϕ is shown to act as a supplementary spectral transfer between both TKE. This spectral transfer is specific to flows in porous media.

Nevertheless, this formal work does not allow us to link the sub-filter production to the work performed by the macro-scale mean flow against the specific mean drag. This link is established by the mean flow energy balance equations. These equations read

$$\begin{aligned}\frac{\mathrm{D}\langle\overline{E}^{\mathrm{M}}\rangle_{\mathrm{f}}}{\mathrm{D}t} &= -\frac{1}{\rho}\frac{\partial\langle\overline{P}\rangle_{\mathrm{f}}\langle\overline{u_i}\rangle_{\mathrm{f}}}{\partial x_i} + \frac{\partial}{\partial x_j}\left(\nu\frac{\partial\langle\overline{E}^{\mathrm{M}}\rangle_{\mathrm{f}}}{\partial x_j}\right) - \nu\frac{\partial\langle\overline{u_i}\rangle_{\mathrm{f}}}{\partial x_j}\frac{\partial\langle\overline{u_i}\rangle_{\mathrm{f}}}{\partial x_j} \\ &\quad - \frac{\partial}{\partial x_j}\langle R_{ij}\rangle_{\mathrm{f}}\langle\overline{u_i}\rangle_{\mathrm{f}} - \underbrace{\left(-\langle R_{ij}\rangle_{\mathrm{f}}\frac{\partial\langle\overline{u_i}\rangle_{\mathrm{f}}}{\partial x_j}\right)}_{\text{transfer to the turbulent motion}} - \frac{\partial}{\partial x_j}\langle\overline{u_i}\rangle_{\mathrm{f}}\langle\delta\overline{u_i}\delta\overline{u_j}\rangle_{\mathrm{f}} \\ &\quad - \underbrace{\left(-\langle\delta\overline{u_i}\delta\overline{u_j}\rangle_{\mathrm{f}}\frac{\partial\langle\overline{u_i}\rangle_{\mathrm{f}}}{\partial x_j} + \langle\overline{u_i}\rangle_{\mathrm{f}}\overline{F_{\phi_i}}\right)}_{\text{transfer to sub-filter mean motion}}, \end{aligned} \tag{20}$$

$$\begin{aligned}\frac{\mathrm{D}\langle\overline{E}^{\mathrm{m}}\rangle_{\mathrm{f}}}{\mathrm{D}t} &= -\frac{1}{\rho}\frac{\partial\langle\delta\overline{P}\delta\overline{u_i}\rangle_{\mathrm{f}}}{\partial x_i} + \frac{\partial}{\partial x_j}\left(\nu\frac{\partial\langle\overline{E}^{\mathrm{m}}\rangle_{\mathrm{f}}}{\partial x_j}\right) - \left\langle\nu\frac{\partial\delta\overline{u_i}}{\partial x_j}\frac{\partial\delta\overline{u_i}}{\partial x_j}\right\rangle_{\mathrm{f}} \\ &\quad - \frac{\partial}{\partial x_j}\langle\delta R_{ij}\delta\overline{u_j}\rangle_{\mathrm{f}} - \underbrace{\left(-\left\langle\delta R_{ij}\frac{\partial\delta\overline{u_i}}{\partial x_j}\right\rangle_{\mathrm{f}}\right)}_{\text{sub-filter production}} - \frac{\partial}{\partial x_j}\langle\delta\overline{E}^{\mathrm{m}}\delta\overline{u_j}\rangle_{\mathrm{f}} \\ &\quad + \underbrace{\left(-\langle\delta\overline{u_i}\delta\overline{u_j}\rangle_{\mathrm{f}}\frac{\partial\langle\overline{u_i}\rangle_{\mathrm{f}}}{\partial x_j} + \langle\overline{u_i}\rangle_{\mathrm{f}}\overline{F_{\phi_i}}\right)}_{\text{transfer from macro-scale mean motion}}. \end{aligned} \tag{21}$$

Now, the macro-scale shear allows an energy transfer from the macro-scale mean motion to both macro-scale and sub-filter turbulent motion. In a similar way, the sub-filter production is an energy transfer from $\langle\overline{E}^{\mathrm{m}}\rangle_{\mathrm{f}}$ to both macro-scale and sub-filter turbulent motion. At the same time, the work performed by the macro-scale mean motion against the drag (which is always a positive term) is a transfer from macro-scale mean motion to sub-filter mean motion.

2.3. Two-scale analysis contribution

The transfer and production terms have been formally derived in the previous section and they are summarized in Fig. 1. By developing Eq. (3), let us emphasize that the sub-filter production is the sum of two contributions,

$$P_{\mathrm{SF}} = -\left\langle\overline{R}^{\mathrm{c}}_{ij}\frac{\partial\delta\overline{u_i}}{\partial x_j}\right\rangle_{\mathrm{f}} - \left\langle(\overline{R}^{\mathrm{m}}_{ij} + \overline{R}^{\mathrm{c}}_{ji})\frac{\partial\delta\overline{u_i}}{\partial x_j}\right\rangle_{\mathrm{f}}, \tag{22}$$

coming from the micro-scale mean flow energy $\langle\overline{E}^{\mathrm{m}}\rangle_{\mathrm{f}}$. Now, in order to simplify kinetic energy exchanges, we shall assume that the micro-scale and macro-scale turbulent motions are weakly correlated. Hence the cross-scale Reynolds tensor and $\bar{k}^{\mathrm{c}}$ shall be neglected (Schiestel, 1987). The macro-scale production is then the sole energy source of $\langle\bar{k}^{\mathrm{M}}\rangle_{\mathrm{f}}$ from the mean flow. By assuming the separation of scales, we also neglect the large eddy creation due to the sub-filter production. The sub-filter production thus reduces to

$$P_{\mathrm{SF}} = -\left\langle\overline{R}^{\mathrm{m}}_{ij}\frac{\partial\delta\overline{u_i}}{\partial x_j}\right\rangle_{\mathrm{f}}. \tag{23}$$

Various scenarii of energy transfers from $\langle\overline{E}^{\mathrm{M}}\rangle_{\mathrm{f}}$ to $\langle\bar{k}^{\mathrm{m}}\rangle_{\mathrm{f}}$ can be considered. For flows in low laden media, the situation is almost the same as for clear flows (see Fig. 2). The shear of the mean macroscopic flow creates macro-scale turbulence. This turbulence is for a part transferred to smaller eddies and then dissipated. The other part, resulting from the eddy fractioning by solids, is transferred to $\langle\bar{k}^{\mathrm{m}}\rangle_{\mathrm{f}}$ through the work performed by the fluctuant macro-scale motion against the fluctuating specific drag (see Fig. 1). For flows in media highly laden with solid structures, the energy transfer follows an opposite way. The macro-scale mean flow quickly yields its energy to the micro-scale one. This transfer is due to the work performed by the mean macro-scale motion against the mean specific drag. Turbulence is then reduced to small structures, supplied by the sub-filter production contribution coming from $\langle\overline{E}^{\mathrm{m}}\rangle_{\mathrm{f}}$.

Fig. 1 schematically illustrates that the influence of the solid inclusions on energy transfers is to create transfers between large scales to small scales. These transfers are related to the drag and to the doubled averaged velocity. In the context of fine-scale turbulence models, the exchange term from mean motion to turbulent motion is related to the shear. In this macro-scale study of turbulence, the macro-scale shear acts in a similar way. We also need to link the sub-filter production, which is induced by the micro-scale shear, to macro-scale quantities and in particular to the drag. However, other transfers than drag contribution supply the micro-scale turbulence. The sub-filter production is then not equal to the work performed by the macroscopic flow against the mean specific drag. In canopy turbulence models, some authors considered that the sub-filter production is conventionally the product between drag and mean macroscopic velocity, minus a sink term. This sink term is supposed to represent the accelerated cascade of TKE due to the plant foliage elements (Green, 1992).

In our approach, considering the limit of a steady homogeneous macroscopic flow with no macroscopic shear, Eq. (20) reduces to

$$P_{\mathrm{SF}} = \overline{F_{\phi_i}}\langle\overline{u_i}\rangle_{\mathrm{f}} - \langle\varepsilon_{\mathrm{w}}\rangle_{\mathrm{f}} \tag{24}$$

with

$$\langle\varepsilon_{\mathrm{w}}\rangle_{\mathrm{f}} = \left\langle\nu\frac{\partial\delta\overline{u_i}}{\partial x_j}\frac{\partial\delta\overline{u_i}}{\partial x_j}\right\rangle_{\mathrm{f}}. \tag{25}$$

As assumed by Green (1992), the sub-filter production may be written as the product between drag and mean macroscopic velocity, minus a sink term. Actually, Eq. (25) shows that this term is a laminar viscous dissipation induced by the velocity deviation gradients. It is important to notice that, in laminar flows, this dissipation is not zero and is strictly equal to the work performed by the mean macroscopic flow against the drag force. According to the mean

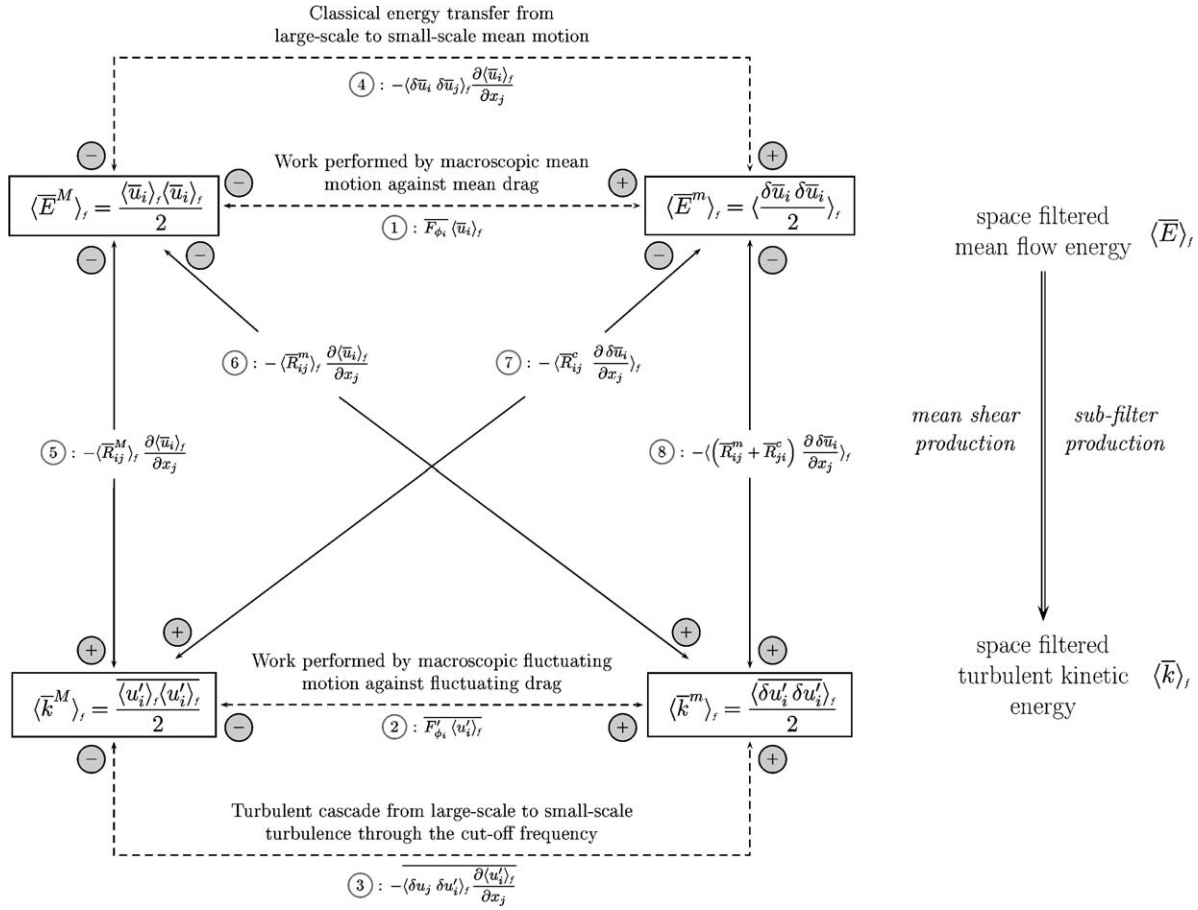

Fig. 1. Schematic description of energy transfers between considered kinetic energies.

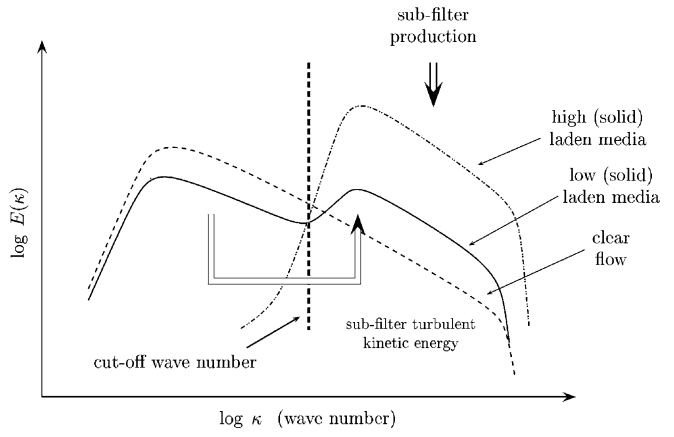

Fig. 2. Schematic spectral representation of turbulence for free flows and flows in porous media.

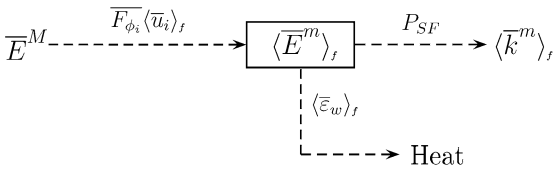

Fig. 3. Schematic description of the $\langle \overline{E}^{m} \rangle_f$ budget under the separation of turbulent scales assumption.

kinetic energy budgets (16)–(20) and under the assumption of separation of the turbulent scales, $\overline{E}^{M}$ provides energy to $\langle \overline{E}^{m} \rangle_f$ by way of the product between drag and double averaged velocity. This amount of energy is not totally transferred to sub-filter turbulence because part of it is directly dissipated into heat by way of laminar wake dissipation. It is illustrated in Fig. 3 that the part received by $\langle \overline{k}^{m} \rangle_f$ from $\langle \overline{E}^{m} \rangle_f$ is the sub-filter production. Thus, in contrast with Green's proposal, we infer that $\langle \overline{\varepsilon}_w \rangle_f$ is reducing the turbulence production instead of increasing the turbulent cascade rate.

3. Derivation of a k–ε model for a stratified porous media

In this section, we choose to analyse one of the simplest medium, say the stratified medium made up by parallel infinite plates. This medium might be seen as a stereotype of the plate heat exchanger. A description of the geometric configuration is given in Fig. 4(a). The turbulent flow is statistically steady, homogeneous in the spanwise x direction and oriented through the z direction. The hydraulic diameter D_H of a channel is twice the clearance between two plates and the Reynolds number of the flow is defined by $Re = \langle \overline{u_z} \rangle_f D_H / \nu$, where $\langle \overline{u_z} \rangle_f$ is the constant bulk flow

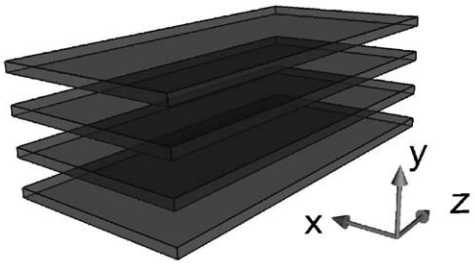

(a) Stratified medium made by parallel infinite plates.

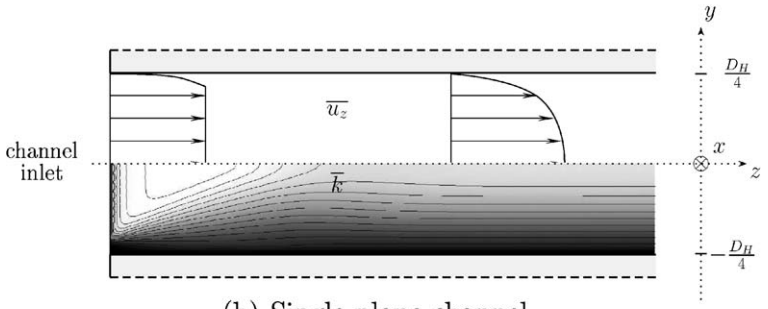

(b) Single plane channel.

Fig. 4. Sketch of the considered stratified medium made by parallel infinite plates. Under the assumptions of homogeneity of the flow in the spanwise x direction and of no macro-scale velocity gradient in the y direction, the medium is approached by a single plane channel. (a) Stratified medium made by parallel infinite plates. (b) Single plane channel.

velocity. No eddies larger than the clearance between two plates can thus exist. Hence, we simply have

$$\langle \bar{k}^{\mathrm{m}} \rangle_{\mathrm{f}} = \langle \bar{k} \rangle_{\mathrm{f}} \quad \text{and} \quad \langle \bar{\varepsilon}^{\mathrm{m}} \rangle_{\mathrm{f}} = \langle \bar{\varepsilon} \rangle_{\mathrm{f}}. \tag{26}$$

In the following developments, we will use the simplest notations. In addition, no velocity gradient exist within the x and y directions, so that macroscopic shear in Eq. (1) vanishes. In such configuration, we approach the stratified medium by a single plane channel (see Fig. 4(b)).

Fine-scale simulations have been performed with the CAST3M CFD code. We use the standard k–ε model (Harlow and Nakayama, 1967; Mohammadi and Pironneau, 1994) with Van Driest wall functions. At the inlet, velocity, TKE and viscous dissipation profiles are flat in the central part of the channel and they follow wall functions in the near wall region. By applying the spatial average to the fine-scale simulation results, we get macroscopic reference evolutions for $\langle \bar{k} \rangle_{\mathrm{f}}$, $\langle \bar{\varepsilon} \rangle_{\mathrm{f}}$, $\langle \bar{\varepsilon}_{\mathrm{w}} \rangle_{\mathrm{f}}$ and the friction factor. Spatially averaged turbulent profiles at the inlet provide channel inlet boundary conditions hereafter denoted by the subscript "0". After a distance of several hydraulic diameters through the z direction, the velocity profile reaches a non-evolving shape and the profiles of $\bar{k}$ and $\bar{\varepsilon}$ reach non-evolving levels and shapes. This state corresponds to the asymptotic state and is hereafter denoted by the subscript "∞". Although the channel inlet boundary conditions are imposed, the asymptotic conditions far dowstream depend on the Reynolds number of the flow. Between inlet and asymptotic states, large scale oscillations of the spatially averaged turbulent quantities are observed (Pinson and Grégoire, submitted for publication).

Fine-scale simulations are classified by using three parameters: the Reynolds number, the ratio $\langle \bar{k}_0 \rangle_{\mathrm{f}} / \langle \bar{k}_\infty \rangle_{\mathrm{f}}$ and the macroscopic turbulent length scale divided by the hydraulic diameter

$$L^*_{tM_0} = \frac{\langle \bar{k}_0 \rangle_{\mathrm{f}}^{3/2}}{\langle \bar{\varepsilon}_0 \rangle_{\mathrm{f}} D_{\mathrm{H}}}. \tag{27}$$

We base the further developments on four cases. We thus consider turbulent flows characterized by

$$\begin{aligned}
&\mathrm{SIM_REF_1}: \quad Re = 10^5, \quad \langle \bar{k}_0 \rangle_{\mathrm{f}} / \langle \bar{k}_\infty \rangle_{\mathrm{f}} = 3, \quad L^*_{tM_0} = 1/10;\\
&\mathrm{SIM_REF_2}: \quad Re = 10^5, \quad \langle \bar{k}_0 \rangle_{\mathrm{f}} / \langle \bar{k}_\infty \rangle_{\mathrm{f}} = 3, \quad L^*_{tM_0} = 1/25;\\
&\mathrm{SIM_REF_3}: \quad Re = 10^5, \quad \langle \bar{k}_0 \rangle_{\mathrm{f}} / \langle \bar{k}_\infty \rangle_{\mathrm{f}} = 3, \quad L^*_{tM_0} = 1/100;\\
&\mathrm{SIM_REF_4}: \quad Re = 5 \times 10^4, \quad \langle \bar{k}_0 \rangle_{\mathrm{f}} / \langle \bar{k}_\infty \rangle_{\mathrm{f}} = 3, \quad L^*_{tM_0} = 1/10.
\end{aligned} \tag{28}$$

The use of wall laws nearby the inlet is not accurate since boundary layer are not enough developed. To assume macroscopic evolution as reference evolution, we have to consider the distance necessary for the boundary layer to develop and to include the non-calculated area. Based on boundary layer thickness increase (Landau and Lifchitz,

1971) we infer that for Reynolds number values considered in this work this condition is achieved past a distance of two hydraulic diameter downstream the inlet.

3.1. Modeled balance equation for $\langle \bar{k} \rangle_f$ and $\langle \bar{\varepsilon} \rangle_f$

In the configuration under study, there is no macro-scale production. Therefore, $\langle \bar{k} \rangle_f$ has a sole production mechanism, that is to say sub-filter production. Diffusion and dispersion of $\langle \bar{k} \rangle_f$ are negligible (Pinson and Grégoire, submitted for publication). Under steady conditions, the $\langle \bar{k} \rangle_f$ balance equation then reads

$$\langle \bar{u}_z \rangle_f \frac{\partial \langle \bar{k} \rangle_f}{\partial z} = P_{SF} - \langle \bar{\varepsilon} \rangle_f. \tag{29}$$

In order to model the sub-filter production P_{SF}, we propose to use the equilibrium relation (24). This model implicitly assume that P_{SF}, $\langle \bar{\varepsilon}_w \rangle_f$ and $\overline{F_{\phi_z}} \langle \overline{u_z} \rangle_f$ are the three major contributions in the $\langle \overline{E}^m \rangle_f$ transport equation. The specific drag force can be related to the friction factor f_p and to the channel hydraulic diameter

$$\overline{F_{\phi_z}} = \frac{f_p}{2D_H} \langle \bar{u}_z \rangle_f^2, \tag{30}$$

so that, according to (24), the sub-filter production can be develop into

$$P_{SF} = \frac{f_p}{2D_H} \langle \bar{u}_z \rangle_f^3 - \langle \bar{\varepsilon}_w \rangle_f. \tag{31}$$

We then postulate a balance equation for $\langle \bar{\varepsilon} \rangle_f$ by analogy with the $\langle \bar{k} \rangle_f$ balance equation (29). Each production/dissipation phenomenum is scaled by a characteristic time scale. The $\langle \varepsilon \rangle_f$ balance equation then reads

$$\langle \bar{u}_z \rangle_f \frac{\partial \langle \bar{\varepsilon} \rangle_f}{\partial z} = C_{\varepsilon_2} \frac{P_{SF}}{\tau_s} - C_{\varepsilon_2} \frac{\langle \bar{\varepsilon} \rangle_f}{\tau_t}. \tag{32}$$

where the time τ_t is defined in accordance with the clear flow modeling

$$\tau_t = \langle \bar{k} \rangle_f / \langle \bar{\varepsilon} \rangle_f, \tag{33}$$

and $C_{\varepsilon_2} = 1.9$. The asymptotic state matches to the zero gradient value of the spatially averaged turbulent quantities:

$$\text{asymptotic state} \iff \frac{\partial \langle \bar{k} \rangle_f}{\partial z} = \frac{\partial \langle \bar{\varepsilon} \rangle_f}{\partial z} = 0. \tag{34}$$

The macroscopic turbulence study in porous media departs from the free turbulence study because of the non-zero asymptotic values of turbulent quantities. The macroscopic model shall allow to recover these values. To this aim, Pinson and Grégoire (submitted for publication) demonstrated that is not possible to set $\tau_s = \tau_t$. A priori testings have shown that the time

$$\tau_s = \tau_t \times (f_{p_\infty}/f_p)^{1/2} \tag{35}$$

is in good agreement with reference results.

To go further, we have to model f_p and $\langle \bar{\varepsilon}_w \rangle_f$. In this work, we will consider that the wake dissipation is a known data (provided by fine-scale simulations), and we focus on the friction factor model for non-equilibrium turbulent flows.

3.2. Modeling of the friction factor f_p for non-equilibrium flows

The friction factor asymptotic value f_{p_∞} may be given by correlations available in the literature, by experimental results, or by fine-scale simulations. Due to the simplicity of the geometry under study, we choose to get the friction factor profiles from fine-scale simulation results. Our aim is to model the friction factor evolution by studying its variations compared to these of $\langle \bar{k} \rangle_f$, $\langle \bar{\varepsilon} \rangle_f$ and $\langle \bar{\varepsilon}_w \rangle_f$.

First of all, we assume that the boundary layer is close to equilibrium. Following Laurence and Boyer (2002), we use the Reichards law to approach the velocity profiles

$$\overline{u_z}(y_w) = u_f g(y^+) \quad \text{with } y^+ = \frac{u_f y_w}{\nu}, \quad \text{and}$$

$$g(y^+) = \frac{1}{0.41} \ln(1 + 0.41 y^+) + 7.8\left(1 - \exp\left(\frac{-y^+}{11}\right) - \frac{y^+}{11} \exp\left(\frac{-y^+}{3}\right)\right), \tag{36}$$

where y_w stands for the distance to the wall and u_f is the friction velocity. In the particular case of the plane channel, pressure contribution to friction is negligible so that the friction velocity is directly linked to the friction factor through

$$u_f = \langle \overline{u_z} \rangle_f (f_p/8)^{1/2}. \tag{37}$$

By calculating the velocity gradient from Eq. (36), using its expression in Eq. (25) and substituting the friction velocity for the friction coefficient, we get

$$\langle \bar{\varepsilon}_w \rangle_f = \frac{f_p^{3/2} \langle \bar{u}_z \rangle_f^3}{D_H} \times \frac{1}{4 \times 2^{1/2}} \int_0^{Re_\tau} \left(\frac{dg}{dy^+}\right)^2 dy^+, \tag{38}$$

where Re_τ is the friction Reynolds number

$$Re_\tau = \frac{u_f D_H}{4\nu}. \tag{39}$$

The function

$$C_w(Re_\tau) = \frac{1}{4 \times 2^{1/2}} \int_0^{Re_\tau} \left(\frac{dg}{dy^+}\right)^2 dy^+ \tag{40}$$

is related to sub-filter velocity gradients (whose highest values are concentrated in a thin region closed to the wall). The integrand in the C_w definition is then very low for large y^+ values. Splitting the integral into two parts, we numerically deduce that for $Re_\tau > 50$, C_w nearly reaches a constant value close to 1.6. Using Eq. (38), we can now define the friction factor asymptotic value as a function of the wake dissipation

$$f_{p_\infty} = \langle \bar{\varepsilon}_{w_\infty} \rangle_f^{2/3} \frac{D_H^{2/3}}{C_w^{2/3} \langle \overline{u_z} \rangle_f^2}. \quad (41)$$

Since Eq. (41), exhibits a direct relation between f_{p_∞} and $\langle \bar{\varepsilon}_{w_\infty} \rangle_f$, we have tempted to extrapolate this asymptotic relation to non-equilibrium states. Unfortunately, it does not work because the velocity profile is not enough close to the Reichard law under far from equilibrium turbulence state. In fact, the wake dissipation acts as an additive dissipation in the $\langle \bar{k} \rangle_f$ balance equation (see Eqs. (29) and (31)). Both $\langle \bar{\varepsilon}_w \rangle_f$ and $\langle \bar{\varepsilon} \rangle_f$ are tightly linked to the velocity profile in the vicinity of walls. Since f_p results from velocity gradients at walls, we thus claim that the friction factor is in fact related to all the amount of dissipation

$$\frac{f_p}{f_{p_\infty}} \simeq \left(\frac{\langle \bar{\varepsilon}_w \rangle_f + \langle \bar{\varepsilon} \rangle_f}{\langle \bar{\varepsilon}_{w_\infty} \rangle_f + \langle \bar{\varepsilon}_\infty \rangle_f} \right)^{2/3}. \quad (42)$$

We have previously underlined that the aim of our model is to reproduce the dynamic of the spatially averaged quantities and to recover the asymptotic state values. However, we demonstrate that, by using the modeled balance equations (29) and (32) (for $\langle \bar{k} \rangle_f$ and $\langle \bar{\varepsilon} \rangle_f$), and by adding the proposed relation (42), the asymptotic value $\langle \bar{k}_\infty \rangle_f$ is undetermined. In following developments, we distinguish the equilibrium state given by the reference data (denoted by the subscript ∞) from the equilibrium state reached by the model (denoted by the subscript $\triangleright$). By writing the modeled balance equations (29) and (32) for their equilibrium state, we get

$$\frac{f_{p\triangleright} \langle \bar{u}_z \rangle_f^3}{2D_H} - \langle \bar{\varepsilon}_{w\infty} \rangle_f - \langle \bar{\varepsilon}_\triangleright \rangle_f = 0, \quad (43)$$

$$C_{\varepsilon 2} \frac{f_{p\triangleright} \langle \bar{u}_z \rangle_f^3 / (2D_H) - \langle \bar{\varepsilon}_{w\infty} \rangle_f}{\tau_{t\triangleright} (f_{p\infty}/f_{p\triangleright})^{1/2}} - C_{\varepsilon 2} \frac{\langle \bar{\varepsilon}_\triangleright \rangle_f}{\tau_{t\triangleright}} = 0. \quad (44)$$

We multiply Eq. (44) by $C_{\varepsilon 2}$ and we subtract the result from Eq. (43):

$$\left(\frac{f_{p_\triangleright} \langle \bar{u}_z \rangle_f^3}{2D_H} - \langle \bar{\varepsilon}_{w_\infty} \rangle_f \right) \left[\left(\frac{f_{p_\infty}}{f_{p_\triangleright}} \right)^{1/2} - 1 \right] \frac{C_{\varepsilon 2}}{\tau_{t_\triangleright}} = 0. \quad (45)$$

Eq. (45) then provides two solutions for the friction factor. These solutions are defined by

$$f_{p\triangleright,1} = \langle \bar{\varepsilon}_{w\infty} \rangle_f \frac{2D_H}{\langle \bar{u}_z \rangle_f^3} \neq f_{p\infty}, \quad (46)$$

and

$$f_{p\triangleright,2} = f_{p\infty}. \quad (47)$$

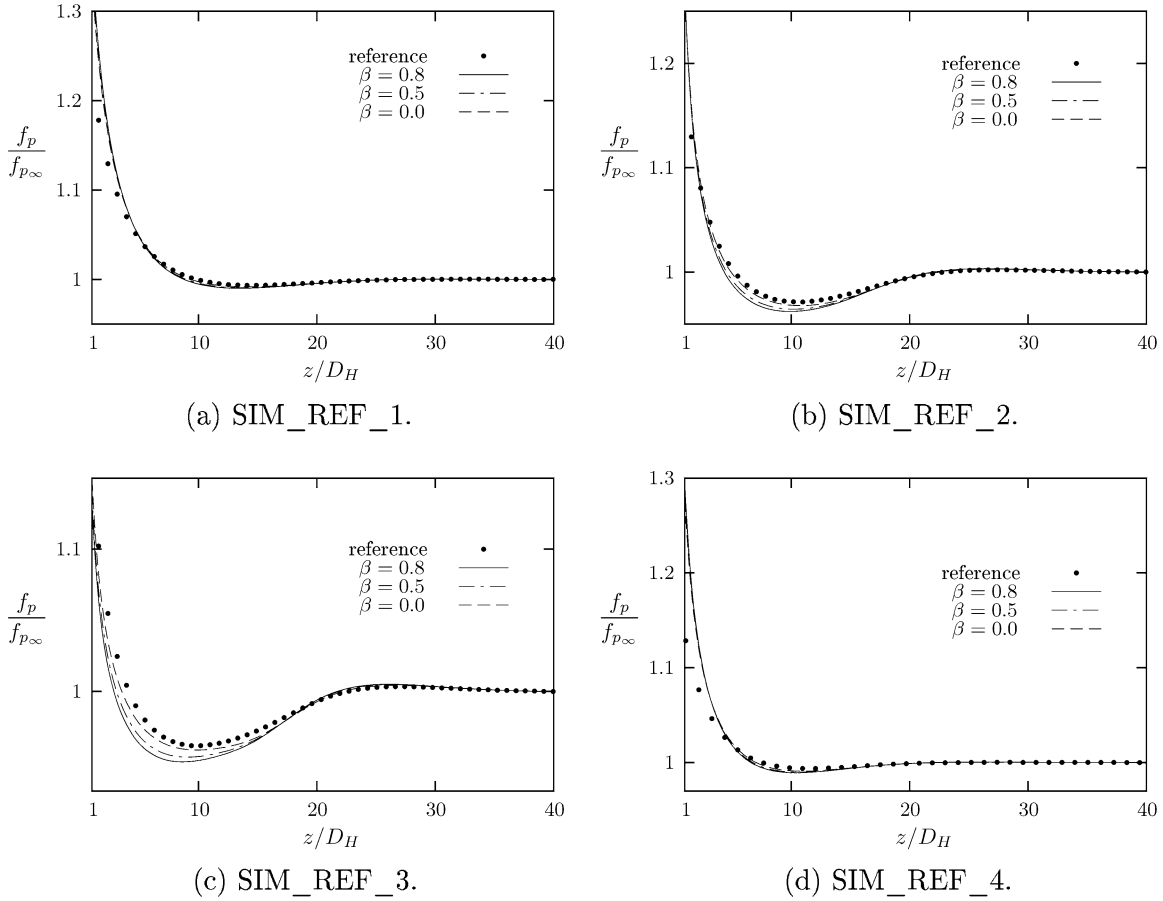

Fig. 5. Friction factor model: comparison between the reference evolution and the expression (50), computed with the reference evolutions of $\langle \bar{k} \rangle_f$, $\langle \bar{\varepsilon} \rangle_f$ and $\langle \bar{\varepsilon}_w \rangle_f$, for different values of the constant β.

Now, we impose the model to provide only one solution corresponding to the reference equilibrium state (∞). The f_p model shall allow the turbulence model to do so. Let us highlight that $f_{p\triangleright,1}$ is related to the following $\langle\bar{\varepsilon}\rangle_f$ value

$$\langle\bar{\varepsilon}_{\triangleright,1}\rangle_f = 0. \tag{48}$$

Nevertheless, by using $f_{p\triangleright,2} = f_{p\infty}$ in Eq. (43), we show

$$\langle\bar{\varepsilon}_{\triangleright,2}\rangle_f = \frac{f_{p\infty}\langle\bar{u}_z\rangle_f^3}{2D_H} - \langle\bar{\varepsilon}_{w\infty}\rangle_f = \langle\bar{\varepsilon}_{\infty}\rangle_f. \tag{49}$$

Whether it is the solution $f_{p\triangleright,1}$ or $f_{p\triangleright,2}$, the $\langle\bar{k}_{\triangleright}\rangle_f$ value is undetermined and consequently not equal to $\langle\bar{k}_{\infty}\rangle_f$. The f_p model might then be improved in order that the complete model allows to reach on one hand only one solution for the friction factor, and on the other hand the asymptotic value $\langle\bar{k}_{\infty}\rangle_f$. We infer that, by adding a corrective factor related to the macro-scale turbulence characteristic velocity non-equilibrium and to the bulk velocity, these drawbacks are corrected. The f_p model reads

$$\frac{f_p}{f_{p_\infty}} \equiv \left(\frac{\langle\bar{\varepsilon}_w\rangle_f + \langle\bar{\varepsilon}\rangle_f}{\langle\bar{\varepsilon}_{w\infty}\rangle_f + \langle\bar{\varepsilon}_{\infty}\rangle_f}\right)^{2/3}\left(1 + \beta\frac{\langle\bar{k}\rangle_f^{1/2} - \langle\bar{k}_{\infty}\rangle_f^{1/2}}{\langle\bar{u}_z\rangle_f}\right), \tag{50}$$

where β is a model constant. To ensure the positivity of the friction factor, the constant β must satisfy the condition:

$$0 \leqslant \beta \leqslant \frac{\langle\bar{u}_z\rangle_f}{\langle\bar{k}_{\infty}\rangle_f^{1/2}}. \tag{51}$$

We compute the relation (50) by using the reference evolutions of $\langle\bar{k}\rangle_f$, $\langle\bar{\varepsilon}\rangle_f$ and $\langle\bar{\varepsilon}_w\rangle_f$, for three values of the parameter β, that is to say $\beta = 0$, 0.5, 0.8. We compare the modeled friction factor (Eq. (50)) with the reference f_p. Fig. 5 shows this comparison for the four simulations described by (28). A good agreement is found, especially in the area where profile shapes are far from their asymptotic shape, for $z/D_H \lesssim 10$. We note that the influence of the parameter β on these quantities is low. Nevertheless, we

Table 1
Description of two $\langle\bar{k}\rangle_f$–$\langle\bar{\varepsilon}\rangle_f$ models for turbulence in a stratified media based on the formulation Eqs. (52) and (53)

	P_{SF}	τ_s	f_p
Model N&K	$P_{SF_\infty} = \langle\bar{\varepsilon}_\infty\rangle_f$	$\tau_{s_\infty} = \langle\bar{k}_\infty\rangle_f/\langle\bar{\varepsilon}_\infty\rangle_f$	f_{p_∞}
Present model	$f_p\langle\bar{u}_z\rangle_f^3/2D_H - \langle\bar{\varepsilon}_w\rangle_f$	$\langle\bar{k}\rangle_f/\langle\bar{\varepsilon}\rangle_f \times (f_{p_\infty}/f_p)^{1/2}$	Given by Eq. (50)

The model of Nakayama and Kuwahara, denoted N&K, and the present model.

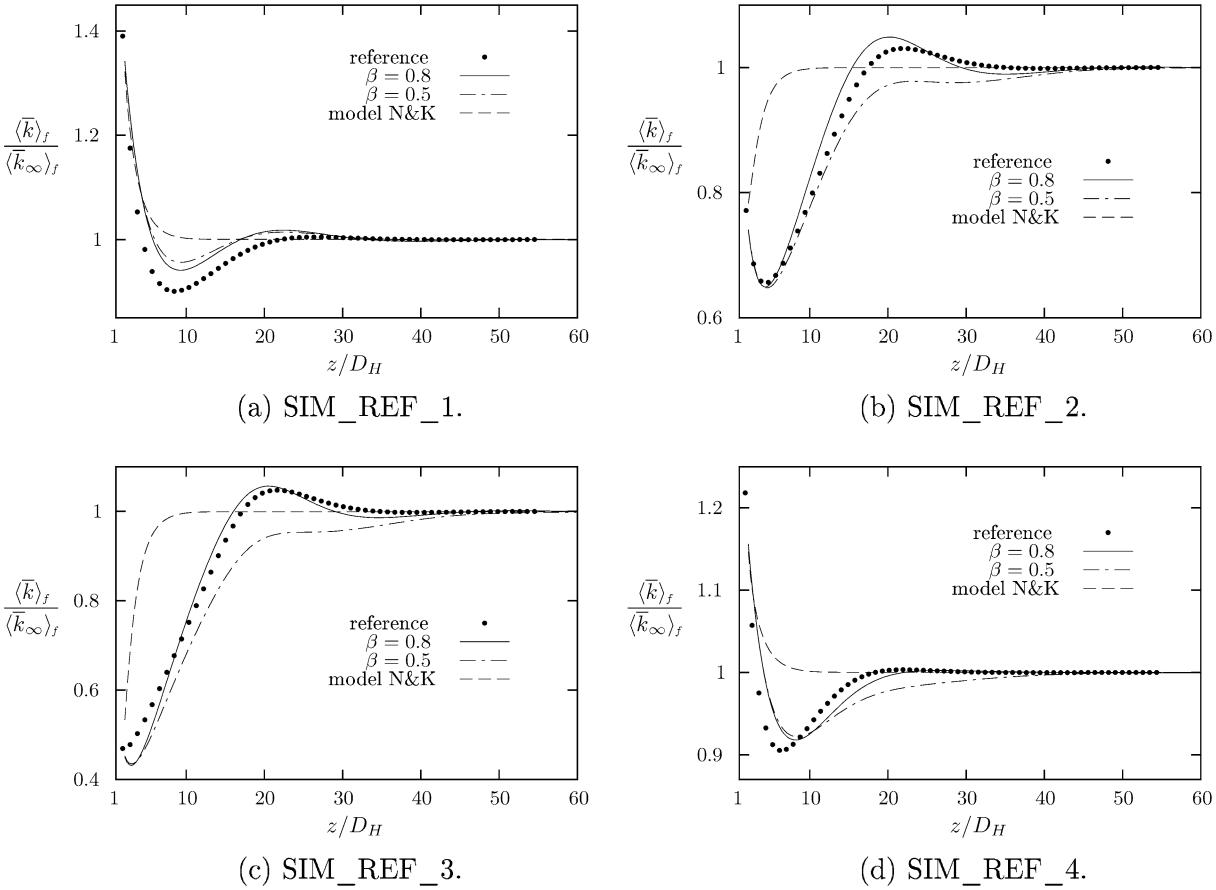

Fig. 6. Macroscopic turbulence models results for turbulent flows in a stratified media: evolution of $\langle\bar{k}\rangle_f$ along the z direction. Comparison between the model described in this paper, the model N&K and reference results.

also underline that the increase in β slightly degrades model results. However, we recall that the choice $\beta = 0$ does not allow the model to reach the asymptotic value $\langle \bar{k}_\infty \rangle_f$.

3.3. Results of the model

Now, results of our present macrosopic turbulence model are compared with spatially averaged fine-scale simulations, described in the introduction of Section 3, and to results of the Nakayama and Kuwahara model (Nakayama and Kuwahara, 1996), hereafter denoted model N&K. This last model is derived for macro-porous ordered media. It includes the modeling of the asymptotic values ($\langle \bar{k}_\infty \rangle_f$ and $\langle \bar{\varepsilon}_\infty \rangle_f$), and also balance equations for $\langle \bar{k} \rangle_f$ and $\langle \bar{\varepsilon} \rangle_f$. Asymptotic values are specifically described for transverse flows in square rod bundles (Nakayama and Kuwahara, 1996). For the flat plate heat exchanger geometry, we cannot use that kind of asymptotic value modeling. However, the modeling of the balance equations in the N&K model is independant of the way asymptotic values are computed. We then use the values obtained from the CAST3M fine-scale simulations. In a steady plane channel, both N&K model and our macroscopic turbulence model reduce to the simple formulation:

$$\langle \bar{u}_z \rangle_f \frac{\partial \langle \bar{k} \rangle_f}{\partial z} = P_{SF} - \langle \bar{\varepsilon} \rangle_f, \tag{52}$$

$$\langle \bar{u}_z \rangle_f \frac{\partial \langle \bar{\varepsilon} \rangle_f}{\partial z} = C_{\varepsilon_2} \left(\frac{P_{SF}}{\tau_s} - \frac{\langle \bar{\varepsilon} \rangle_f}{\tau_t} \right), \tag{53}$$

where τ_t is given by (33). Table 1 summarizes the discrepancies between the two models, based on the formulation (52) and (53). Once the stratified media is seen as an homogeneous media thanks to the spatial average application, the formulation of the $\langle \bar{k} \rangle_f$–$\langle \bar{\varepsilon} \rangle_f$ model is comparable to the formulation of the grid turbulence decay. Supplementary terms, related to the sub-filter production, account for the solid structures action on turbulence. Nakayama and Kuwahara (1996) argued that these terms are constant and equal to their asymptotic values. This implies that turbulence is close to equilibrium within the overall domain. In the model presented in this paper, these terms vary and part of their modeling has been carried out.

Simulations of macroscopic evolutions of $\langle \bar{k} \rangle_f$ and $\langle \bar{\varepsilon} \rangle_f$ are performed using a one-dimensional code based on a finite volume upwind scheme. Source terms are fully explicit. We recall that the wake dissipation $\langle \bar{\varepsilon}_w \rangle_f$ is given by the spatially averaged fine-scale simulations. Hence, comparisons presented here might be seen as a priori tests. The fric-

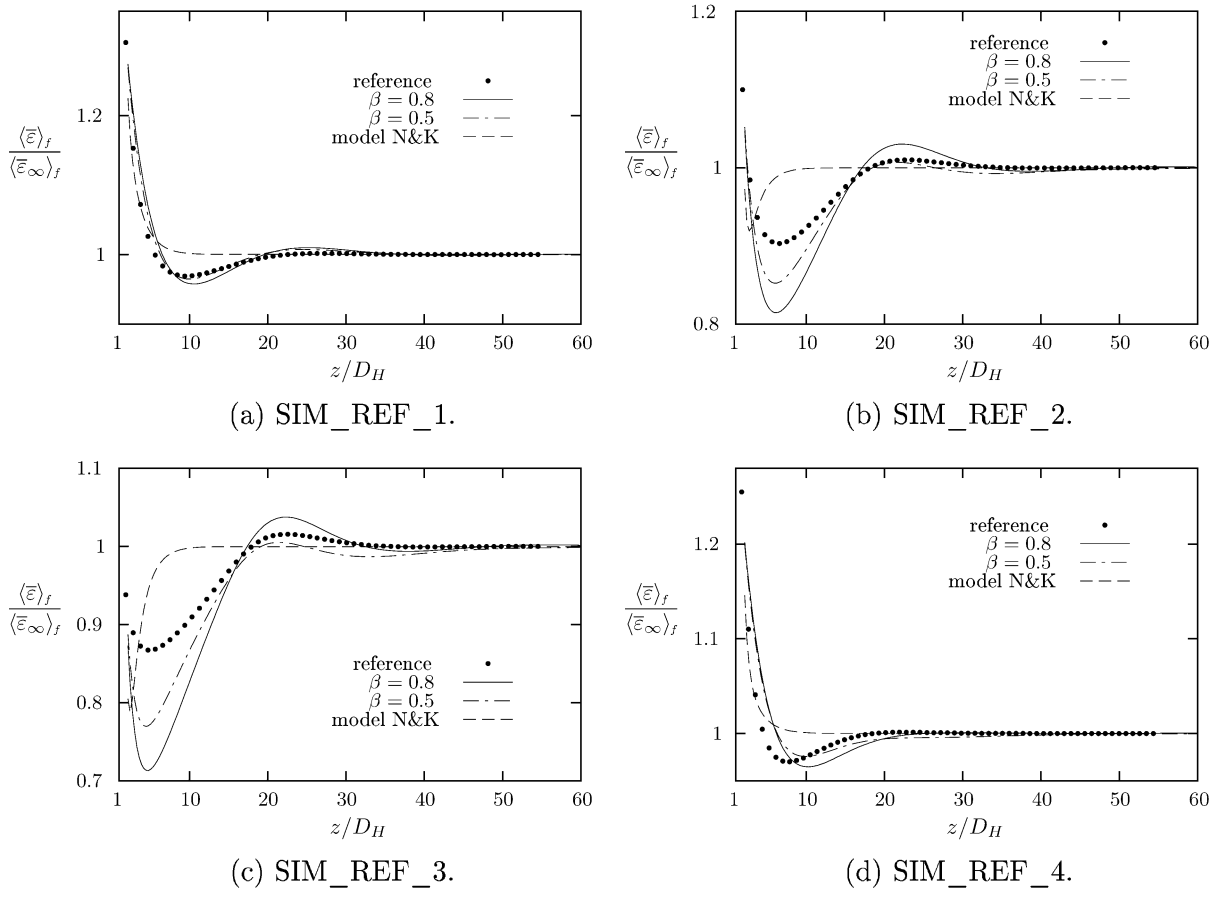

Fig. 7. Macroscopic turbulence models results for turbulent flows in a stratified media: evolution of $\langle \bar{\varepsilon} \rangle_f$ along the z direction. Comparison between the model described in this paper, the model N&K and reference results.

tion factor is deduced from Eq. (50). The simulation domain starts at $z/D_H = 2$ and ends at $z/D_H = 60$. A uniform grid composed by two hundred cells is used. At the inlet of the simulated domain, a Dirichlet boundary condition is applied by using the reference values at this point. At the end of the simulated domain, we consider that the asymptotic state is reached and we then applied a Neumann boundary condition. Convergence tests on mesh grid and time step have been performed. Results presented here are fully converged. Comparisons between the present model, the model N&K and reference results are carried out by studying the evolutions of $\langle\bar{k}\rangle_f/\langle\bar{k}_\infty\rangle_f$, $\langle\bar{\varepsilon}\rangle_f/\langle\bar{\varepsilon}_\infty\rangle_f$ and f_p/f_{p_∞}. To do so, we lean on the four test cases corresponding to the description (28).

The model N&K then exhibits in all cases a rapid relaxations to the asymptotic state (Figs. 6 and 7). By setting the solid action model terms to their asymptotic values, the competitions between the sub-filter production P_{SF} and the viscous dissipation $\langle\bar{\varepsilon}\rangle_f$ on one hand, and between their characteristic time scales on the other hand, are too much simplified. To assume P_{SF} constant (and equal to its asymptotic value) is equivalent to assume a velocity profile close to establishment. In the studied configuration, this hypothesis is clearly false over twenty to thirty hydraulic diameters downstream the channel inlet. In addition, by choosing the time τ_s equal to its asymptotic value, Nakayama and Kuwahara guarantee that the model recover the $\langle\bar{k}_\infty\rangle_f$ and $\langle\bar{\varepsilon}_\infty\rangle_f$ values. But in the same way, they also assume that the time τ_t remains nearly constant. That assumption is clearly not achieved here.

We now focus on the results provided by the model introduced in this paper. We note that the choice of the time τ_s added to the friction factor model allow our model to recover the dynamic behavior of the $\langle\bar{k}\rangle_f$ and $\langle\bar{\varepsilon}\rangle_f$ evolutions (Figs. 6 and 7). We can now analyse the discrepancies existing between the reference and our model results. At the inlet, $\langle\bar{k}\rangle_f$, $\langle\bar{\varepsilon}\rangle_f$ and $\langle\bar{\varepsilon}_w\rangle_f$ are imposed equal to fine-scale results. Nevertheless, for the cases SIM_REF_1 and SIM_REF_4, the f_p model provides values which are higher than reference values (Fig. 8(a) and (d)). It induces an overestimation of the ratio between P_{SF} and τ_s. Hence, the modeled $\langle\bar{\varepsilon}\rangle_f$ decreases more slowly than the reference one. At the contrary, for the cases SIM_REF_2 and SIM_REF_3, the f_p model provides values which are lower than reference values. The ratio P_{SF}/τ_s is underestimated and the modeled $\langle\bar{\varepsilon}\rangle_f$ decreases more rapidly than the reference one. The model construction, and especially the τ_s expression, allows to counterbalance this effect. Now, let us underline that an overestimation of the friction factor at the starting point of the macroscopic simulation has lower consequences on the evolution of the friction factor than an underestimation.

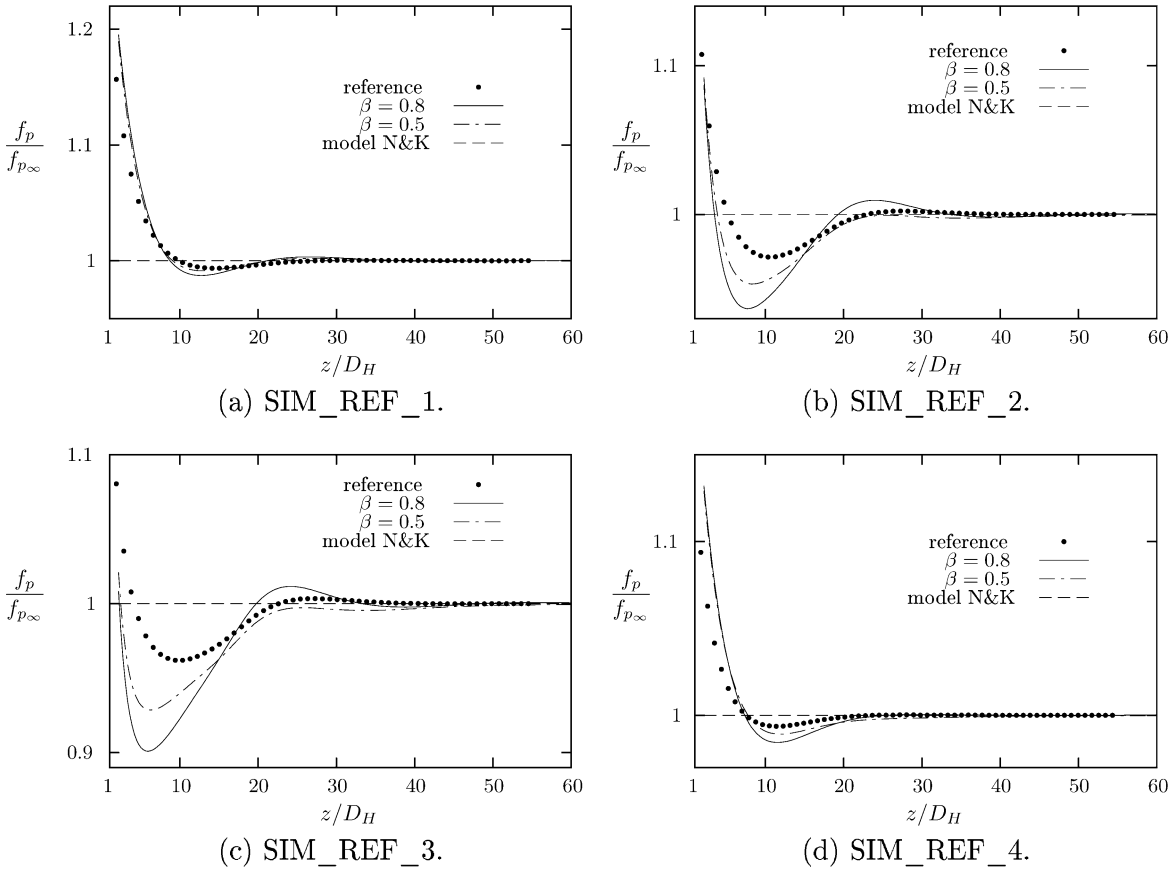

Fig. 8. Friction factor model results for turbulent flows in a stratified media. Comparison between the model (50) described in this paper, the model N&K and reference results.

We also underline that, once the f_p model (50) is coupled with the $\langle\bar{k}\rangle_f$–$\langle\bar{\varepsilon}\rangle_f$ model, the parameter β has a high influence on each evolution. This observation is in contrast with the one done in the previous section and shows again how sensible the coupling is: increasing β involves oscillations with a larger amplitude.

Lastly, we propose some ways to improve this modeling. We recall that for these a priori tests, we have used the reference evolution of the wake dissipation. Nevertheless, a relevant model shall not refer to any reference evolution. In forthcoming work, a balance equation for the wake dissipation should be derived. The identification of the source/sink terms of $\langle\bar{\varepsilon}_w\rangle_f$, and their caractéristic time scales, would allow us to postulate a balance equation for this quantity. At the same time, we will work on a model for the asymptotic values. We will then check that the same modeling methodology could apply to other non-detached flows, such as flows in tube or flows in rod bundle parallel to the main direction of the geometry.

4. Conclusion

In this paper, we have derived a macro-scale turbulence model for flows embedded in a solid matrix. Due to the spatial averaging procedure, numerous terms need to be closed. To do so, a formal two-scale analysis has been carried out to put forward each transfer existing within the turbulent motion and the mean motion in a porous medium. According to this analysis, the sub-filter production is described thanks to the product between the drag of the solid structures and the double averaged velocity, minus a wake dissipation. We then study the macroscopic evolution of a turbulent flow in a stratified medium made by parallel infinite plates. Using $\langle\bar{k}\rangle_f$, $\langle\bar{\varepsilon}\rangle_f$ and $\langle\bar{\varepsilon}_w\rangle_f$ coming from fine-scale simulation results, we perform a priori tests in order to derive a dynamical closure for the friction factor. Considering that the wake dissipation evolution is a known data, our $\langle\bar{k}\rangle_f$–$\langle\bar{\varepsilon}\rangle_f$ model depends on only one parameter: β. Comparisons with results provided by the N&K model exhibit significant improvements. Possible ways of improvement have also been suggested.

Acknowledgements

This work has been performed with the financial support from the Direction de la Propulsion Nucléaire of the CEA (CEA/DAM/DPN).

References

Antohe, B.V., Lage, J.L., 1997. A general two-equation macroscopic turbulence model for incompressible flow in porous media. Int. J. Heat Mass Transfer 40, 3013–3024.

Breugem, W.P., Boersma, B.J., 2005. Direct numerical simulations of turbulent flow over a permeable wall using a direct and a continuum approach. Phys. Fluids, 17.

de Lemos, M.J.S., Braga, E.J., 2003. Modeling of turbulent natural convection in porous media. Int. Commun. Heat Mass Transfer, 30.

Finnigan, J., 2000. Turbulence in plant canopies. Ann. Rev. Fluid Mech. 32, 519–571.

Getachew, D., Minkowycz, W.J., Lage, J.L., 2000. A modified form of the k–ε model for turbulent flows of an incompressible fluid in porous media. Int. J. Heat Mass Transfer 43, 2909–2915.

Green, S.R., 1992. Modelling turbulent air flow in a stand of widely-spaced trees. PHOENICS J. Comput. Fluid Dyn. Appl. 5, 294–312.

Grégoire, O., Souffland, D., Gauthier, S., Schiestel, R., 1999. A two-time-scale turbulence model for compressible flows: turbulence dominated by mean deformation interaction. Phys. Fluids 11, 3793–3807.

Harlow, F.H., Nakayama, P.I., 1967. Turbulence transport equations. Phys. Fluids 10 (11), 2323–2332.

Landau, L., Lifchitz, E., 1971. Physique théorique 6: Mécanique des Fluides. éditions MIR.

Laurence, D., Boyer, V., 2002. A shape function approach for high- and low-Reynolds near-wall turbulence model. Int. J. Numer. Meth. Fluids 40, 241–251.

Mohammadi, B., Pironneau, O., 1994. Analysis of the *K*–Epsilon Turbulence Model. John Wiley & Sons, Masson.

Nakayama, A., Kuwahara, F., 1996. A macroscopic turbulence model for flow in a porous medium. J. Fluid Eng.—T ASME 121, 427–433.

Nield, D.A., 2001. Alternative models of turbulence in a porous medium, and related matters. J. Fluid Eng.—T ASME 123, 928–931.

Pedras, M.H.J., de Lemos, M.J.S., 2001. Macroscopic turbulence modeling for incompressible flow through undeformable porous media. Int. J. Heat Mass Transfer 44, 1081–1093.

Pinson, F., Grégoire, O., Simonin, O., submitted for publication. Macroscale turbulence modeling for flows in media laden with solid structures. C.R. Acad. Sci. Paris, Série 2 .

Quintard, M., Whitaker, S., 1994a. Transport in ordered and disordered porous media I: The cellular average and the use of weighting functions. Transport Porous Med. 14, 163–177.

Quintard, M., Whitaker, S., 1994b. Transport in ordered and disordered porous media II: Generalized volume averaging. Transport Porous Med. 14, 179–206.

Reynolds, W.C., Langer, C.A., Kassinos, S.C., 2002. Structure and scales in turbulence modeling. Phys. Fluids 14 (7), 2485–2492.

Schiestel, R., 1987. Multiple-time-scale modeling of turbulent flows in one-point closure. Phys. Fluids A—Fluid 30 (3), 722–731.

Silva, R.A., de Lemos, M.J., 2003. Turbulent flow in a channel occupied by a porous layer considering the stress jump at the interface. Int. J. Heat Mass Transfer, 46.

Travkin, V.S., 2001. Discussion: Alternative models of turbulence in a porous medium, and related matters (D.A. Nield, 2001, J. Fluid Eng.—T ASME 123, pp. 928–931). J. Fluid Eng.—T ASME 123, 931–934.

Vu, T.C., Ashie, Y., Asaeda, T., 2002. A k–ε turbulence closure for the atmospheric boundary layer including urban canopy. Bound.-Layer Meteorol. 102, 459–490.

Whitaker, S., 1967. Diffusion and dispersion in porous media. AIChE 13 (3), 420–427.